Replication Stress-mediated Regulation of Nuclear Actin Filament

Weijie Liao

Wolfson College

Department of Oncology

University of Oxford

Supervisor: Professor Eric O'Neill

A thesis submitted for the degree of Master of Science (by Research) in Oncology

October 2024

Acknowledgements

I would like to express my deepest gratitude to my supervisor, Dr. Eric O'Neill, for his guidance both in research and in life. His sense of humour and his high standards in scientific research have left a lasting impression on me. My heartfelt thanks also go to Simei Go, whose invaluable advice on my research and meticulous revisions of my paper were essential to its completion. Without her patient guidance, this paper would not have been possible.

I am also deeply thankful to Tess Stanly for her crucial suggestions during my experiments, and to Alice Evans, Giampiero Valenzano, Ben Futcher, and everyone else in the lab for their support and assistance throughout my research journey. Special thanks to Joanne Russell for helping me settle into life in Oxford, her kindness and patience were much appreciated.

I would also like to thank my two Chinese friends, Chenwan Jin and Xiaosheng Zhu, who traveled to Oxford with me and provided tremendous support both in my research and in daily life. Lastly, I am deeply grateful to my parents for their unwavering support as I pursued my studies abroad, and to myself for staying resilient and committed throughout this journey.

Content

1. Abstract

The Hippo pathway is a critical regulator of proliferation and cell fate during development. This pathway can transmit cellular signals via the RASSF1-6 and Sav1 scaffold proteins to the MST and LATS kinases, which further regulate chromatin and the transcriptional activity of YAP/TAZ. However, the specific mechanisms by which the Hippo pathway influences events within the nucleus remain unclear.

ATR is a key regulatory kinase that responds to replication stress and is also believed to be an important mediator of nuclear events in response to mechanical stress signals. Our previous research has shown that under mechanical stress, ATR is recruited to the nuclear envelope and acts upstream of RASSF1A, mediating its phosphorylation and ultimately promoting the formation of nuclear actin filaments.

Actin filaments are a transient state of actin assembly, playing significant roles in mechanical support, mechanical signal transduction, and intracellular transport. While most actin is cytoplasmic, nuclear actin is involved in various physiological processes, including the response to replication stress, where the formation of nuclear actin filaments (NAFs) is thought to facilitate the translocation of stress replication sites to the nuclear periphery, though the

exact mechanisms are not fully understood. Given ATR's dual role in responding to both replication and mechanical stress, we aimed to investigate whether ATR and RASSF1A exhibit similar mechanisms under replication stress to promote the formation of NAFs.

Our results demonstrate that HeLa cells stimulated with hydroxyurea (HU) generate a state of replication stress and lead to the formation of NAFs. Immunofluorescence revealed that ATR was not recruited to the nuclear envelope upon HU treatment, but was diffusely distributed within the nucleus. Over prolonged HU treatment, ATR formed complexes with RPA32 and eventually migrated towards the nuclear envelope. Concurrently, phosphorylated RASSF1 at the nuclear envelope increased. Through immunoprecipitation and immunofluorescence, we found that inhibition of ATR with VE-821 resulted in a decrease in NAFs, along with reduced RASSF1A binding to filamin A and decreased levels of phosphorylated RASSF1. SiRNA knockdown of RASSF1A also inhibited NAFs formation and HU-induced RPA32 aggregation. These results suggest that under replication stress, ATR may participate in the phosphorylation of RASSF1A, and by promoting the phosphorylation of RASSF1A and its binding to filamin A, facilitates the formation of nuclear actin filaments, thereby aiding the translocation of replication stress sites to the nuclear periphery.

Key words: replication stress, RASSF1A, nuclear actin filament, ATR.

2. Introduction

2.1 Dual Role of ATR

Ataxia-telangiectasia mutated- and Rad3-related (ATR), belonging to the phosphatidylinositol 3-kinase-related kinase protein family, is regarded as an essential regulator in the DNA damage response [1]. When DNA damage occurs, replication protein A (RPA) is recruited on single-strand DNA (ssDNA). At the 5′-ended ssDNA–double-stranded DNA (dsDNA) junction adjacent to the Okazaki fragment, the RAD17–RFC2-5 clamp loader facilitates the loading of the RAD9–RAD1–HUS1 (9-1-1) clamp complex onto the DNA. Subsequently, the 9-1-1 complex, in conjunction with the RHINO protein and the MRE11–RAD50–NBS1 (MRN) complex, recruits the ATR activator TOPBP1 (topoisomerase II binding protein 1), thus activating ATR pathway for further DNA damage repairing [2]. For instance, checkpoint kinase 1 (CHK1) is phosphorylated by activated ATR to induce replication stress response [3]. Besides, ATR is involved in resolution of torsional stress induced by chromatin replication during S phase. Mec1/ATR pathway participates in regulation of chromatin detachment from the nuclear envelope (NE) as replication forks approach chromatin domain related to the NE, and thus resolve aberrant topological transitions and promote fork progression [4]. This raises the question about how ATR senses the chromatin behaviour during replication fork movement.

In fact, ATR can sense mechanical force from both inside and outside. Experimental induction of mechanical stress, including osmotic changes, cell stretching, and compression, triggers the reversible relocalisation of ATR to the NE, independent of DNA damage signaling. This response is mediated through the activation of Chk1, ATR's downstream kinase, and occurs within physiological force ranges [5]. Internal force like torsional stress from chromosomal dynamics can also cause NE location of ATR [5]. However, the mechanism of how ATR relocates to NE and how ATR is regulated as a mechanical sensor during this process remains unclear.

2.2 Function of Nuclear Actin Filament in Replication Stress

Actin filaments are a transient state of actin assembly, playing significant roles in mechanical support, mechanical signal transduction, and intracellular transport [6]. While most actin is cytoplasmic, nuclear actin is involved in various physiological processes, including the response to replication stress and chromatin organization [7-9]. In response to replication stress， ATR kinase, which activates mTORC1, leads to the nucleation of nuclear actin through IQGAP1, WASP, and ARP2/3. This process is specific to S phase and occurs concurrently with fork stalling, indicating its role in the replication stress response [9, 10]. The formation of nuclear actin filaments results in significant alterations to nuclear architecture, including increased nuclear volume and

sphericity [10]. These changes counteract nuclear deformation caused by replication stress, providing a more stable environment for DNA metabolism and replication fork repair [10]. Besides, nuclear actin filament, in conjunction with myosin II, enhances the mobility of stressed replication foci, promoting their movement towards the nuclear periphery [10]. Though the exact mechanisms of formation of nuclear actin filaments are not fully understood.

2.3 Distribution, Epigenetic Features of RASSF1A in Cancer

The Hippo pathway is a critical regulator of proliferation and cell fate during development [11]. Scaffold protein Ras association domain family (RASSF) plays an essential role in hippo pathway with ten family members, RASSF1-10 [12]. RASSF1A, an isoform of RASSF1， is widely studied and transmits cellular signals to the Hippo kinases MST and LATS kinase, which further regulate chromatin and the transcriptional activity of YAP/TAZ [13].

RASSF1A is frequently inactivated in various cancers through epigenetic modifications, particularly promoter hypermethylation [14]. This gene, located on chromosome 3p21.3, is often subject to allelic loss in lung and breast cancers, making it a focal point for cancer research [14]. In non-small-cell lung cancer (NSCLC), RASSF1A messenger RNA (mRNA) is absent in 65% of cell lines and 30% of primary tumours [14]. Similarly, in small-cell lung cancer (SCLC), RASSF1A is not expressed in 100% of cell lines [14]. In breast cancer,

RASSF1A expression is missing in 60% of cell lines and 49% of primary tumours [14]. This widespread loss of expression suggests a critical role for RASSF1A in tumour suppression across different cancer types.

The primary mechanism of RASSF1A inactivation in cancer is promoter hypermethylation. In NSCLC, 63% of cell lines and 30% of primary tumours exhibit RASSF1A promoter hypermethylation. In SCLC, all cell lines (100%) show hypermethylation, while in breast cancer, 64% of cell lines and 49% of primary tumours have hypermethylated RASSF1A promoters [14]. Importantly, this hypermethylation is not observed in nonmalignant lung tissues, indicating that it is a cancer-specific event [14].

2.4 Role of RASSF1A and pRASSF1A in Nuclear Actin Filament Formation

The phosphorylation status of RASSF1A is crucial for its tumour suppressor activity. Two key phosphorylation sites in RASSF1A, Ser131 and Ala133, play crucial roles in its function. The Ser131 site is a putative substrate for the ATM kinase, which is involved in DNA damage response and cell cycle regulation [15]. And both S131F and A133S mutation reduce RASSF1A phosphorylation, diminishing its capacity to block cyclin D1 accumulation and cell cycle progression [15]. Notably, the A133S mutation, identified in some tumour samples, is a single nucleotide polymorphism (SNP) that affects RASSF1A's phosphorylation state [14].

The O'Neill lab has previously shown that Ser131 phosphorylation of RASSF1A is related to the formation of nuclear actin filament in response to high osmotic pressure (unpublished data). Interestingly, in response to mechanical stress, ATR is recruited to the NE and acts as the upstream activator of this process, inducing Ser131 phosphorylation of RASSF1A [16].

The formation of NAFs plays a critical role in responding to both mechanical and replication stress. Since ATR and RASSF1A promote NAFs formation under mechanical stress, and ATR has dual roles in mechanical and replication stress, we aimed to investigate whether similar mechanisms promote NAFs formation under replication stress.

3.Method

3.1 Cell Culture and Treatment

Hela cells were cultured in DMEM complete medium, supplemented with 10% heat inactivated (HI) fetal bovine serum (FBS) and 1X penicillin streptomycin and 1% L-glutamine. All cells were maintained in a cell incubator at 37°C with 5% CO_2. HU (MCE #127-07-1) and VE-821 （MCE #1232410-49-9）, at concentrations of 2 mM and 1 μM respectively, were selectively added to the culture medium as required by the experimental design.

3.2 BCA Assays and Protein Sample Preparation

Protein concentration was measured using a BCA assay kit （Thermo Fisher Scientific #23225）. The BCA protein standards were diluted with RIPA buffer （Thermo Fisher Scientific #89900） to concentrations of 2000, 1000, 500, 250, 125, 62.5, 31.25, and 15.625 μg/ml. The BCA working solution was prepared at a ratio of 50:1 of reagent A to reagent B, with 200 μL added to each well of a 96-well plate. The experimental samples were diluted 5-fold with water, and 10 μL of each sample was added to the wells. Similarly, 10 μL of the protein standard solutions were added to the respective wells. The plate was then incubated at 37°C for 30 minutes, and the absorbance at 562 nm was measured using a microplate reader. The protein concentration of the experimental samples was determined by interpolation from the standard curve.

To prepare samples for SDS-PAGE, a defined amount of protein was mixed with NuPAGE LDS Sample Buffer (Invitrogen #NP0007, at a final concentration of 1X) and dithiothreitol (DTT, MCE #3483-12-3, 1 mM final concentration), then adjusted to a consistent volume using ddH_2O. The samples were briefly centrifuged before and after boiling at 95°C for 10 minutes.

3.3 Western Blot

SDS-PAGE Gel Electrophoresis:

In this experiment, 3 to 8% NuPAGE™ Tris-Acetate Mini Protein Gels

（Invitrogen #EA03785BOX），PageRuler Prestained Protein Ladder (10-180 kDa, Thermo Scientific #26617) and PageRuler Plus Prestained Protein Ladder (10-250 kDa， Thermo Scientific #26619) were used. After assembling the gel and the electrophoresis tank, 1X NuPAGE MOPS SDS Running Buffer （Invitrogen #NP000102） was added, ensuring that the buffer fills the space between the gel plates. Allow the setup to sit and check for any leakage before loading the samples. The electrophoresis was run at a constant voltage of 130V to separate proteins based on their molecular weights. The running time was determined based on the desired molecular weight of the target protein, with complete separation typically requiring around 90 minutes.

Membrane Transfer:

A 0.45 mm polyvinylidene difluoride (PVDF) membrane was used. Prior to transfer, immerse the membrane in methanol for 15 seconds, then wash it twice in transfer buffer (192 mM glycine, 25 mM Tris, 10% methanol, diluted in ddH_2O) on a shaker. The gel was arranged in a "transfer sandwich" with layers consisting of sponge-3 layers of filter paper-gel-PVDF membrane-3 layers of filter paper-sponge. This sandwich was placed into the electrophoresis tank, and 1X transfer buffer was added. Transfer was performed at a constant voltage of 30V for 60 minutes.

Blocking:

The membrane was placed in 5% non-fat milk, which wasdissolved in TBST (50 mM Tris, 150 mM NaCl, pH 7.6, 0.1% Tween-20, diluted in ddH_2O) and blocked on a shaker for 1 hour at room temperature.

Antibody Incubation:

After blocking, wash the membrane with TBST three times, then incubate with the primary antibody for 2 hours at room temperature or overnight on a shaker at 4°C. The next day, wash the membrane with TBST three times for 5 minutes each, followed by incubation with the secondary antibody for 1 hour at room temperature. After incubation, wash the membrane twice with TBST and once with ddH_2O, each for 5 minutes.

Detection:

Mix the enhanced chemiluminescence (ECL) substrate solutions A and B in a 1:1 ratio, and evenly apply the mixture to the membrane for chemiluminescent detection. In this experiment, Immobilon Western Chemiluminescent HRP Substrate was used. The images was captured using a Biorad Chemidoc.

3.4 Immunofluorescence

Sterilized coverslips (18 mm, #1.5, SLS) were placed into a 12-well plate, with one coverslip in each well. Then, $1x10^5$ cells were seeded into each well and shaken to distribute the cells evenly. After 24 hours, when the cell confluence

reached 90%, cells were incubated with 2 mM HU at different timepoints. Following incubation, the culture medium was discarded, and the cells were washed three times with phosphate-buffered saline (PBS). Cells were fixed with 4% paraformaldehyde (PFA) at room temperature for 15 minutes, followed by three washes with PBS. The coverslips were then immersed in PBS solution and stored at 4°C overnight.

The next day, samples were blocked in blocking buffer (3% BSA with 0.3% Triton in PBS solution) at room temperature for 30 minutes. Primary antibodies were prepared by dissolving in blocking buffer at the following dilutions: ATR at 1:200, pRASSF1 at 1:50, and other antibodies at 1:100. A total of 25 µL of the antibody mixture was applied as droplets on parafilm. The cell-coated side of the coverslips was placed face down on the antibody droplets and incubated at 37°C for 1 hour. After incubation, the coverslips were washed three times with PBS, each time on a shaker for 5 minutes. The same procedure was followed for secondary antibody incubation at 1:2000 dilution, followed by washing.

Finally, 5 µL of SlowFade Diamond Antifade Mountant （Invitrogen #S36963）was placed on a microscope slide for each coverslip, and the cell-coated side of the coverslip was mounted on the mountant. The coverslip was sealed with Coverslip Sealant. The slides were then ready for observation under Zeiss 780 Confocal microscope using a 63X objective lens.

3.5 Plasmid Transfection

As an example, using a 12-well plate, on the first day, seed 1×10^5 HeLa cells per well, adding 1 mL of DMEM medium containing 10% FBS and antibiotics. On the second day, once the cells reached 70-90% confluence, replace the medium with DMEM containing FBS but without antibiotics. Meanwhile, prepare the transfection solution. For each well, 0.75 μg of plasmid, 4.5 μg of PEI, and 100 μL of DMEM without antibiotics and FBS were required. The plasmid and PEI should be prepared separately in DMEM in different centrifuge tubes, allowed to stand for 5 minutes, and then mixed to form the transfection solution. After waiting for 10 minutes, add 100 μL of the transfection solution to each well. Six hours later, replace the medium with DMEM containing 10% FBS but without antibiotics to remove any residual transfection components, and continue culturing for 12 hours before proceeding to the next experiment.

3.6 SiRNA Knockdown

Cells were plated at a density of 2×10^5 cells per well in a 6-well plate and incubated overnight at 37°C. For siRNA transfection, a siRNA mixture was prepared by combining 10 μL of siRNA stock solution (20 μM) with 190 μL of antibiotic- and serum-free medium (Opti-MEM or serum-free DMEM) and incubating for 5 minutes at room temperature. In parallel, a RNAiMAX (Invitrogen # 13778030) mixture was prepared by adding 7.5 μL of RNAiMAX

reagent to 193.5 µL of Opti-MEM for each condition, followed by a 5-minute incubation. The siRNA mixture was then combined with 200 µL of the RNAiMAX mixture, yielding a total volume of 400 µL, and incubated for 20 minutes to allow complex formation.

The medium was aspirated from the cells, and the wells were washed twice with PBS. Subsequently, 1.6 mL of antibiotic-containing medium supplemented with 10% FBS was added to each well, followed by the addition of 400 µL of the siRNA-RNAiMAX complex. Cells were incubated for 24 hours, after which the medium was replaced with either standard growth medium or growth medium containing specific treatments. Gene knockdown was expected to occur between 48 and 72 hours post-transfection.

SiRNA sequence against RASSF1A is: GACCUCUGUGGCGACUU.

3.7 Antibodies

For western blot:

Antibody	**Concentration**	**Cat.**	**Company**
pSer131-RASSF1	1:500	custom made	Eurogentec
RASSF1A	1:1000	86026	Cell Signaling
ATR	1:500	2790	Cell Signaling
MST2	1:1000	ab52641	Abcam

pCHK1 (S345)	1:1000	2348S	Cell Signaling
CHK1	1:1000	sc-8408	Santa Cruz
RPA32	1:1000	2208S	Cell Signaling
Vinculin	1:1000	4650S	Cell Signaling
β-actin	1:1000	60008-1-1g	Proteintech
Filamin A	1:1000	4762S	Cell Signaling
anti-mouse IgG, HRP-linked	1:5000	7076	Cell Signaling
anti-rabbit IgG, HRP-linked	1:5000	7074	Cell Signaling
anti-rat IgG, HRP-linked	1:5000	7077	Cell Signaling

For immunofluorescence:

Antibody	**Concentration**	**Cat.**	**Company**
ATR	1:200	2790	Cell Signaling
RASSF1A	1:100	86026	Cell Signaling
pSer131-RASSF1	1:50	custom made	Eurogentec
RPA32	1:100	2208S	Cell Signaling
Goat anti-rabbit 647	1:2000	A-21244	Invitrogen
Goat anti-rabbit	1:2000	A-11011	Invitrogen

568			
Goat anti-mouse 647	1:2000	A28181	Invitrogen
Goat anti-mouse 568	1:2000	A-11031	Invitrogen
Goat anti-rat 488	1:2000	A-11006	Invitrogen

For Immunoprecipitation:

Anti-RASSF1A antibody (Invitrogen, eB114-10H1) was used.

3.8 Immunoprecipitation

The cells were washed twice with pre-chilled PBS to remove excess culture medium. Using the back of a pipette tip, the cells were gently scraped in a clockwise direction from the outer edge to the center of the culture dish. The collected liquid was centrifuged at 300 g for 5 minutes at 4°C to obtain the cell pellet. The supernatant was discarded, and 400 µL of pre-chilled NP-40 buffer (50 mM Tris (pH 7.5), 150 mM NaCl, 1.0 mM EDTA, 1% NP-40) was added to the pellet. The mixture was gently pipetted to resuspend the cells, then placed on ice for at least 60 minutes for lysis, with gentle mixing every 10 minutes.

The lysate was then centrifuged at 16,000 g for 10 minutes at 4°C. The supernatant was collected, with 40 µL set aside as the input sample, and samples were processed directly for Western blot or stored at -80°C. The

remaining 360 μL of the supernatant was used for immunoprecipitation (IP). To each IP sample, 2 μg of RASSF1A antibody was added, and the mixture was incubated overnight at 4°C with rotation.

The next day, Protein G magnetic beads were added to each IP sample in equal amounts, and the mixture was incubated at room temperature with rotation for 30 minutes. The tubes were then placed on a magnetic rack for magnetic separation. The liquid was carefully aspirated along the non-magnetic side to avoid accidental removal of the beads. The beads were washed three times with PBST by rotating for 5 minutes, with magnetic separation and liquid removal performed after each wash. After the final wash, the liquid was removed on the magnetic rack, and the samples were placed on a regular tube rack. Samples were mixed with NuPAGE LDS Sample Buffer (at a final concentration of 1X) and dithiothreitol (DTT, 1 mM final concentration), then adjusted to a consistent volume using ddH_2O. The samples were briefly centrifuged before and after boiling at 95°C for 15 minutes to elute the proteins bound to the beads for further downstream analysis.

4. Result

4.1 Hydroxyurea-Induced Replication Stress Activates the ATR pathway in Hela Cells.

To investigate the relationship between ATR, RASSF1A, and nuclear actin

filaments, we first aimed to establish a replication stress model. Here we used hydroxyurea (HU), a non-competitive inhibitor of ribonucleotide reductase that significantly reduces deoxyribonucleotide levels, thereby blocking DNA synthesis, inhibiting replication fork progression, and arresting cells in the S phase of the cell cycle. To establish this replication stress model in Hela, we first treated cells with HU at a final concentration of 2 mM for 0, 2, 4, and 6 hours, and confirmed whether HU induces replication stress and activates the ATR-mediated pathway using Western blot and immunofluorescence.

Our results showed that with increasing HU treatment duration, pCHK1 levels progressively increased, and a higher molecular weight of RPA32 appeared at 4 hours of treatment, which is indicative of phosphorylation of RPA (Figure 1a). The activation of pCHK1 and pRPA32 are indicative of activation of the ATR-mediated pathway. Additionally, immunofluorescence images revealed that RPA32 formed numerous foci as well as some nuclear envelope (NE)-localized foci after 4 hours of HU treatment, suggesting the formation of replication stress sites within the nucleus [17] (Figure 1b). These findings demonstrate that we successfully established an HU-mediated replication stress model, capable of effectively activating the ATR-mediated pathway.

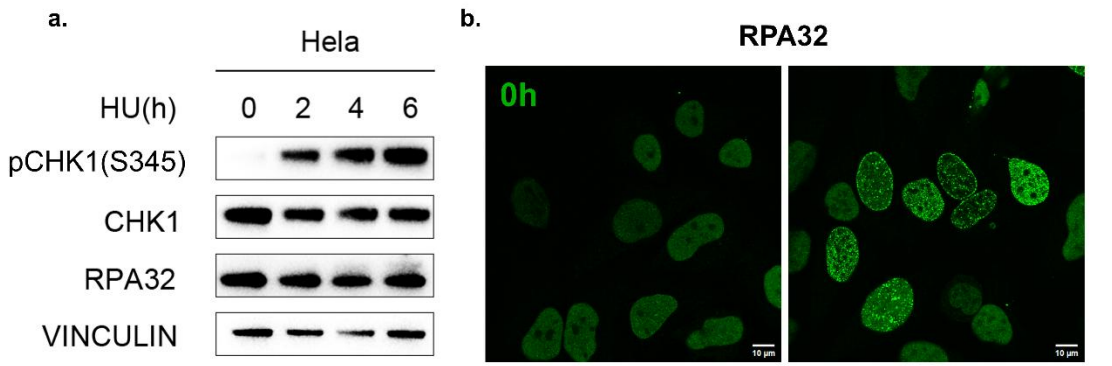

Figure 1: Hydroxyurea induces replication stress and activates the ATR pathway in Hela cells.

a, WB analysis was performed on whole cell lysates collected from Hela cells treated with 2 mM HU for 0, 2, 4, and 6 hours. n = 3 biological replicates. **b**, IF analysis of RPA32 was performed on Hela cells treated with 2 mM HU for 0 and 4 hours. Cells were fixed with PFA for 20 minutes. **b** is a representative figure of n = 3 biological replicates. Scale bars = 10 μm.

4.2 Hydroxyurea-Induced Formation of Nuclear Actin Filaments Is Time-Dependent in HeLa Cells.

After successfully establishing the replication stress model, we next aimed to see whether replication stress induces nuclear actin filaments. Since actin filaments are abundantly present in the cytoplasm, direct immunofluorescent staining makes it difficult to distinguish cytoplasmic from nuclear actin filaments. To address this, we used ChromoTek Nuclear Actin-Chromobody® plasmid (TagGFP), which encodes anti-Actin VHH (anti-actin Nanobody) tagged with TagGFP2 and a nuclear localisation signal (NLS). Theoretically, anti-Actin VHH

will localize to the nucleus, bind to actin and emit a green fluorescent signal, which can be observed under a confocal microscope.

Our results showed successful expression of the plasmid in HeLa cells, with the majority of the green fluorescent signal concentrated in the nucleus (Figure 2a). Additionally, we quantified the proportion of successfully transfected cells with NAFs after HU treatment at different time points. The results indicated that the proportion of cells with NAFs was highest after 4 hours of HU stimulation, but decreased at 6 hours, suggesting that 4 hours is a critical time point for NAFs formation (Figure 2b). This finding is consistent with the RPA32 phosphorylation timing observed in Figure 1. Although previous studies have measured the proportion of cells with NAFs after 6 hours of HU treatment, the author used in that study was the population of cells in the S phase [10]. The 6-hour data suggest that the process of NAFs formation under HU treatment is likely time-dependent and that a certain mitigation mechanism may be established between 4 and 6 hours.

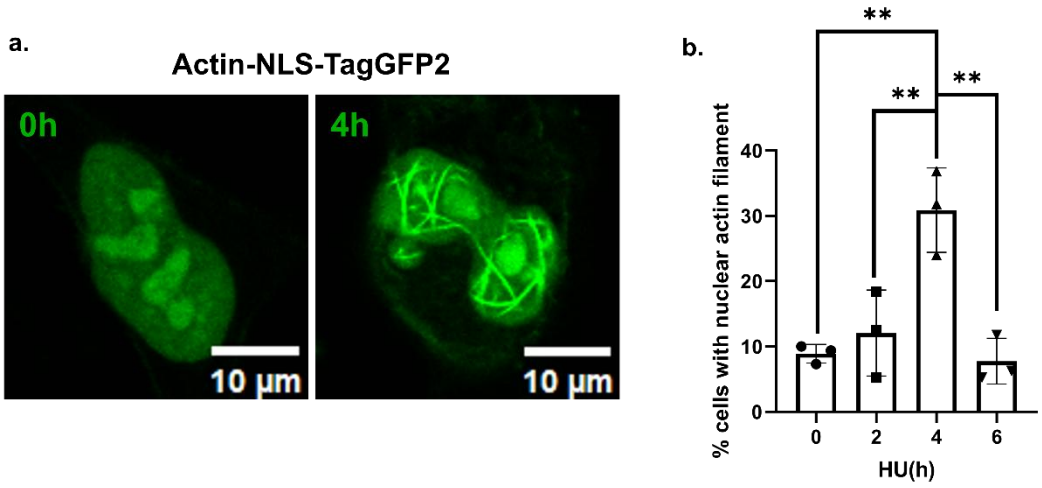

Figure 2: Hydroxyurea induces formation of nuclear actin filaments in Hela cells.

a, IF analysis was performed on Hela cells transfected with ChromoTek Nuclear Actin-Chromobody® plasmid (TagGFP) to overexpress nuclear-localized actin. After 2 mM HU treatment for 0 and 4 hours, cells were fixed with paraformaldehyde (PFA) for 20 minutes. **a** is a representative figure of n = 3 biological replicates. Scale bars = 10 μm. **b**, Quantification of the percentage of successfully transfected Hela cells expressing nuclear actin filaments. n = 3 biological replicates from **a**. The significance of the data was determined using one-way ANOVA. **P<0.01.

4.3 Hydroxyurea-Mediated Replication Stress Promotes Nuclear Envelope Localisation of RPA32, ATR and pRASSF1A.

The aggregation of RPA32 at ssDNA sites and its recruitment of ATR, leading to hyperphosphorylation of RPA32, represents a key mechanism in the response to DNA damage. In the earlier part of this study, we observed the

formation of RPA32 foci and their NE localization, suggesting a possible tendency for RPA32 to migrate toward the NE. However, it remains unclear whether ATR exhibits a similar migration pattern and whether this NE localisation could promote interaction between ATR and RASSF1A. To further investigate the dynamic changes of RASSF1A, ATR, and RPA32 under replication stress and explore potential mechanisms, we used IF to simultaneously label ATR, Lamin B1, RPA32, and DAPI, or Lamin A/C, RASSF1A, RPA32, and DAPI, or Lamin A/C, pRASSF1A, RPA32, and DAPI. Lamin B1 and Lamin A/C were used as a marker for the nuclear envelope. We found that after 4 hours of HU treatment, both ATR and RPA32 formed foci, and by 6 hours, both partially co-localized with Lamin B1 (Figure 3a,3d). There was no significant change in the nuclear distribution of RASSF1A, which was mainly on NE (Figure 3b). However, the integrated fluorescence intensity of RASSF1A on the NE slightly decreased at 4 hours, suggesting that there might be a loss of RASSF1A from the nuclear envelope or a reduction in its expression level at this time (Figure 3e). Additionally, the NE localisation of pRASSF1A was observed only at 4 hours of HU stimulation, which is consistent with the previously observed timing of NAFs formation, whereas at 0 and 6 hours, it exhibits a scattered distribution within the nucleus (Figure 3c, 3d, 3f). These findings suggest that HU-mediated replication stress promotes the aggregation and NE localisation of RPA32 and ATR, and the localisation of pRASSF1A is likely closely related to the formation of NAFs.

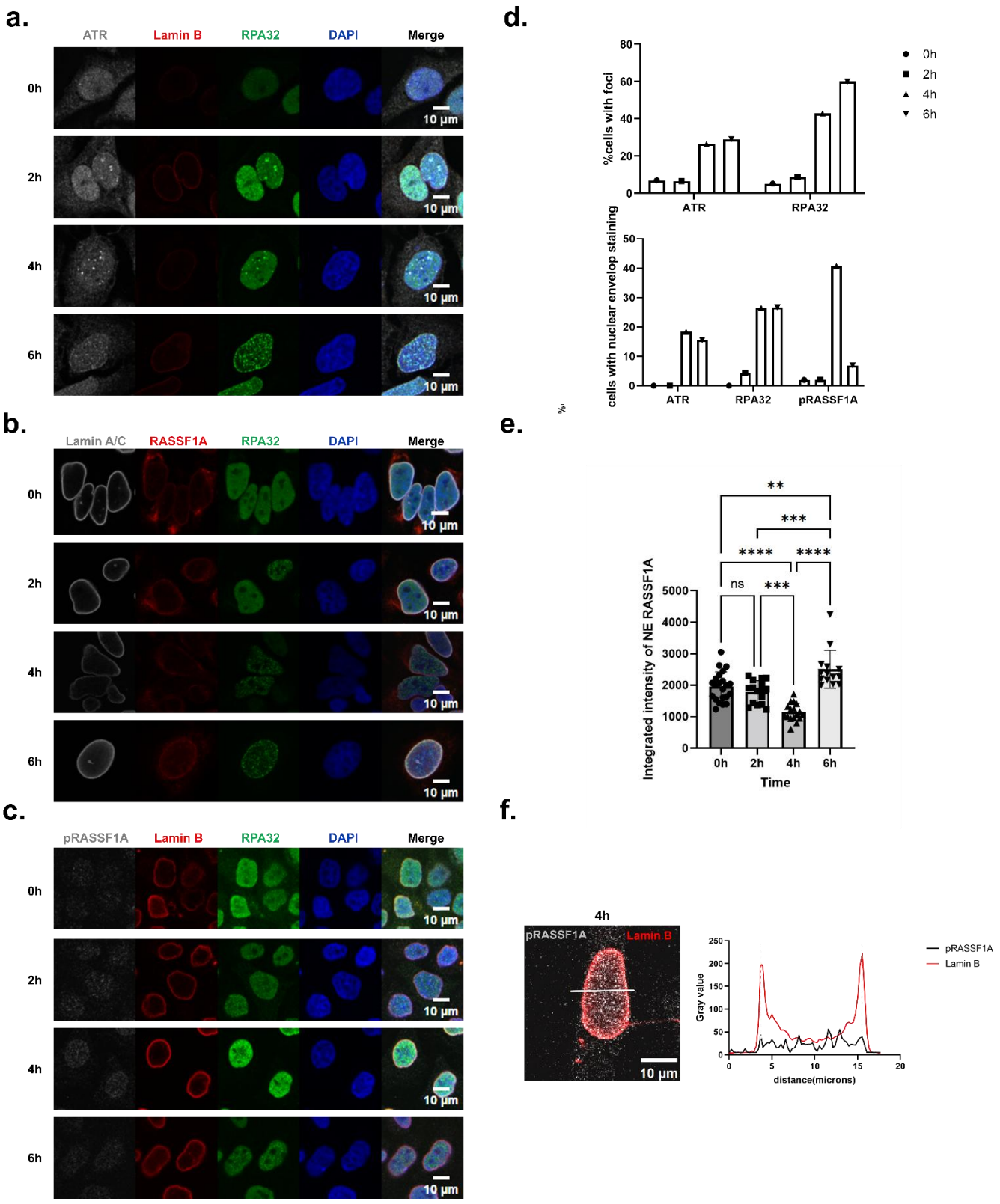

Figure 3: Hydroxyurea induces translocation of RPA32, ATR and pRASSF1A to the nuclear envelope in Hela cells.

a-c, IF analysis was performed on Hela cells treated with 2mM HU for 0, 4 and 6 hours. Cells were fixed with paraformaldehyde (PFA) for 20 minutes. n = 2 biological replicates for **a-c**, respectively. **d**, Quantification of the percentage of Hela cells expressing ATR and RPA32 foci and Hela cells expressing nuclear envelop-localized ATR, RPA32 and phosphorylated RASSF1A (pRASSF1A). Hela cells were treated with 2 mM HU for 0, 2, 4 and 6 hours. n=1. **e**, Quantification of the integrated intensity of NE RASSF1A. Hela cells were treated with 2 mM HU for 0, 2, 4 and 6 hours. n=2. **f**, Fluorescence intensity profile of Lamin B (red) and pRASSF1A (black) signals across the HeLa nuclei. Overlapping peaks in the figure indicated by white dashed lines (right). Position of line scan indicated by the white line (left). **f** is a representative figure of n = 2 biological replicates. Scale bars = 10 μm.

4.4 Inhibition of ATR Reduces RASSF1A-Filamin A Interaction and Suppresses Nuclear Actin Filaments Formation Under Replication Stress.

To further investigate the molecular mechanisms involved in the formation of NAFs, we used the ATR inhibitor VE-821 at a final concentration of 1 μM to inhibit ATR activation. Previous research has identified Filamin A through a proteomics screen as a protein that binds to pRASSF1A, while MST2 has been shown to mediate RASSF1A's NE localization [18]. Therefore, we focused on analysing Filamin A, Actin, and MST2 to further understand their roles in RASSF1A dynamics during NAFs formation. We performed IF and co-IP to

analyse NAFs formation and protein interactions under ATR inhibition. We found that, in the absence of VE-821, 4 hours of HU treatment significantly promoted the binding of RASSF1A to Filamin A and Actin, with no changes in its interaction with MST2 (Figure 4a). Since RASSF1A NE localization is dependent on MST2, this observation aligns with the fact that HU treatment does not alter RASSF1A localization (Figure 3b). Surprisingly, pRASSF1A showed almost no change, indicating that the proportion of pRASSF1A relative to total RASSF1A did not significantly change under HU stimulation (Figure 4a). However, in the presence of VE-821, after 4 hours of HU treatment, the binding of RASSF1A to Filamin A, Actin, and MST2 was significantly reduced, and pRASSF1A levels also decreased, indicating a reduction in the proportion of pRASSF1A relative to total RASSF1A (Figure 4a). Statistical analysis of HeLa cells with NAFs in the immunofluorescence assay further demonstrated that VE-821 reduced the proportion of HeLa cells with NAFs under HU stimulation compared with Figure 2b (Figure 4c). However, VE-821 alone induced NAFs formation in cells without HU treatment, which may be attributed to the inherent cytotoxicity of VE-821 (Figure 4c). It should be noted that there was a lack of control groups without HU but containing VE-821 at all the time points. As shown in Figure 2b and Figure 4, these findings suggest that ATR activation promotes NAFs formation under HU-induced replication stress.

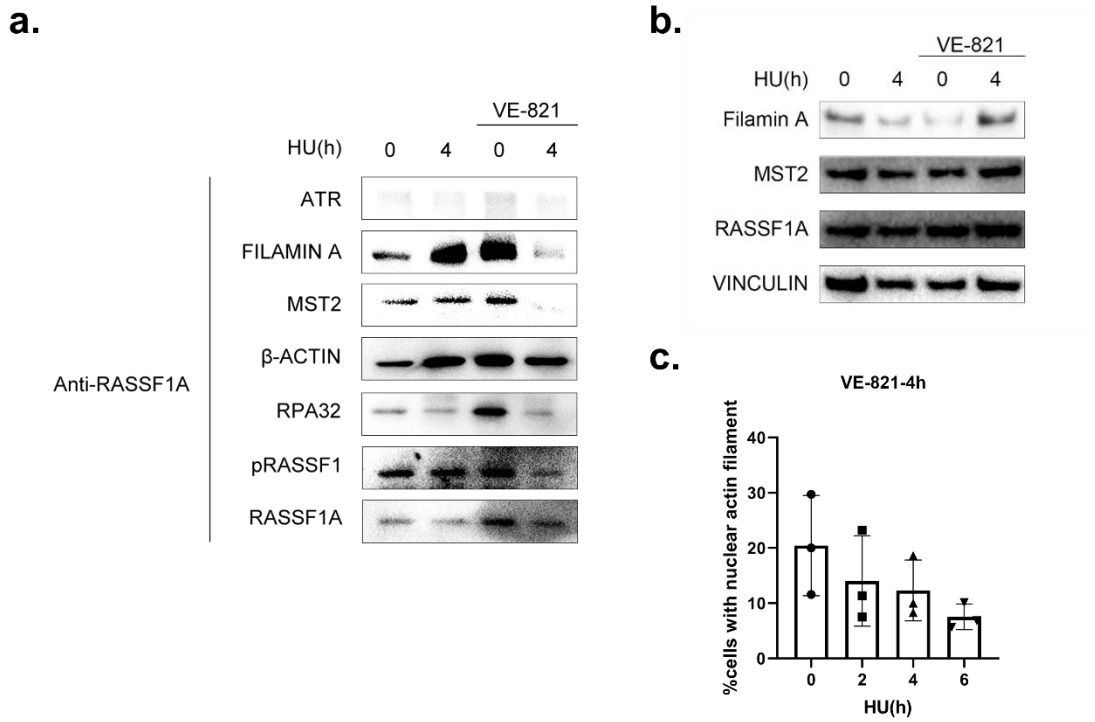

Figure 4: Inhibition of ATR suppresses the formation of nuclear actin filaments in Hela cells.

a, IP experiments were performed using anti-RASSF1A antibody. One set of experiments involved treating Hela cells with 2 mM HU for 0 and 4 hours. In another set, cells were treated with 2 mM HU for 0 and 4 hours, concurrently with 1 μM ATR inhibitor VE-821 for 4 hours. **b**, Input of samples from **a** was performed using anti-VINCULIN, anti-RASSF1A, anti-MST2 and anti-Filamin A antibody. **c**, Quantification of the percentage of successfully transfected Hela cells expressing nuclear actin filament. Hela cells were treated with VE-821 for 4 hours. Additionally, cells were subjected to 2 mM HU treatment for 0, 2, 4, and 6 hours. n = 2 biological replicates for **a-c**.

4.5 SiRNA knockdown of RASSF1A inhibits Nuclear Actin Filaments

formation and HU-induced RPA32 Aggregation.

To further confirm whether RASSF1A plays a role in NAFs formation, we used RASSF1A-targeting small interfering RNA (siRNA). WB analysis confirmed a reduction in RASSF1A expression following siRNA treatment (Figure 5a). IF assays were then performed on both siRNA-treated and untreated cells. We found that, despite 4-hour HU treatment, the proportion of transfected cells with NAFs was similar to that of untreated cells (Figure 5b, 5c). However, due to the oversight in the experimental arrangement and the tight scheduling of time, the control groups with negative control of siRNA and HU were missing in Figure 5b. Additionally, the percentage of cells with RPA32 foci showed no significant difference between HU-stimulated and non-stimulated groups (Figure 5c). Notably, reduced RASSF1A expression led to an increase in Filamin A expression, which may serve as a compensatory mechanism for the loss of RASSF1A (Figure 5a). These results suggest that RASSF1A plays a critical role in NAFs formation and may also influence HU-induced RPA32 foci formation.

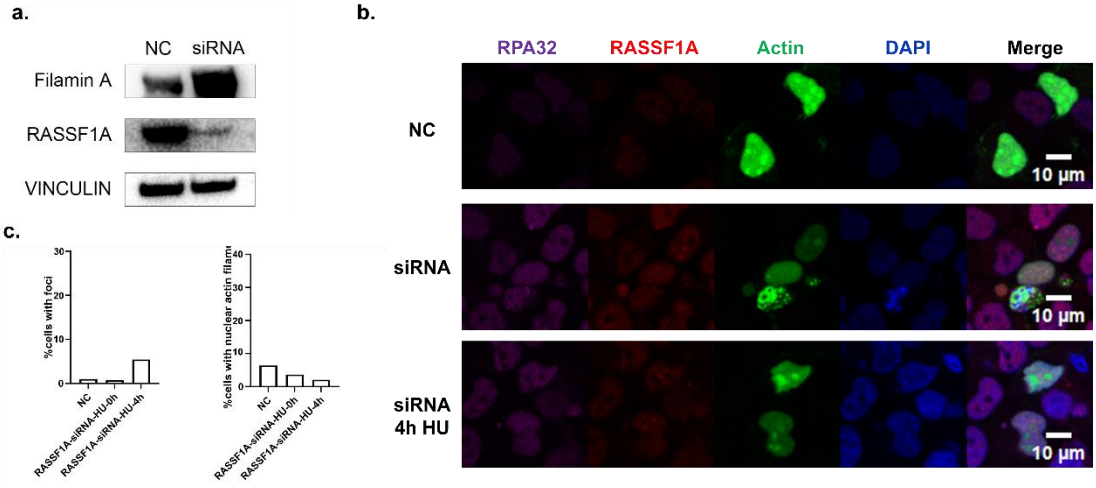

Figure 5: SiRNA knockdown of RASSF1A suppresses formation of NAFs

and RPA32 foci.

a, WB experiments were performed to check RASSF1A-siRNA efficiency using anti-RASSF1A, anti-VINCULIN, anti-Filamin A antibody. **b**, IF analysis was performed on Hela cells treated with negative control of siRNA or RASSF1A-siRNA or RASSF1A-siRNA with 2mM HU for 4 hours. Cells were fixed with PFA for 20 minutes. **c**, Quantification of the percentage of Hela cells expressing NAFs or RPA32 foci. Hela cells were treated as b. n = 1 for **a-c.**

5. Discussion

RASSF1A, as a key component of the Hippo signaling pathway, plays a significant role in various conditions, including cardiovascular diseases, kidney diseases, and cancer [19]. Therefore, understanding what physiological processes it regulates and how RASSF1A interacts with proteins such as ATR is of great importance. Our previous experiments have demonstrated that ATR activation plays a crucial role in formation of NAFs after 4 hours of HU stimulation. Given that ATR has been shown to phosphorylate RASSF1A under cellular stress (i.e. hyperosmotic conditions or DNA damage), our next step is to investigate whether RASSF1A phosphorylation play a critical role in ATR-regulated NAFs formation under HU stimulation. To directly investigate whether RASSF1A phosphorylation is crucial for NAFs formation, generation of a HeLa cell line with a serine 131 phosphorylation site mutation in RASSF1A using CRISPR-Cas9 technology could be generated. By comparing NAFs formation

between the mutant and non-mutant cell lines under HU stimulation conclusions can be drawn whether RASSF1A phosphorylation is critical for NAFs formation.

The dynamic spatiotemporal behaviour of various proteins involved in DNA damage repair has been a critical area of research. In this study, we also focused on the process of replication stress-induced DNA damage repair, which involves dynamic trafficking of ATR, RPA32, and RASSF1A to the nucleoplasm and NE. We observed that ATR and RPA32 form foci during HU stimulation, and that a proportion of cells demonstrate NE staining after 4 hours of HU treatment. This is in line with the process of damaged chromosomal regions moving to the nuclear periphery to facilitate DNA repair [9, 10]. However, RASSF1A itself did not show strong colocalisation with ATR or RPA32 foci in this process. Instead, phosphorylated RASSF1A exhibited NE localisation after 4 hours of HU stimulation, which coincides with the highest proportion of cells with NAFs observed at that time point. And the proportion of pRASSF1A relative to total RASSF1A did not significantly change under HU stimulation. However, in the presence of VE-821, an ATR inhibitor, after 4 hours of HU treatment, pRASSF1A levels decreased. If RASSF1A and its phosphorylation indeed play a critical role, the question is how RASSF1A and its phosphorylation contribute to NAFs formation. We hypothesize that RASSF1A maintains a stable level of phosphorylation under normal conditions, while ATR, in response to HU stimulation, plays a crucial role in the translocation and sustained

phosphorylation of pRASSF1A as it aggregates and moves toward the nuclear envelope. Additionally, during the early stages of HU stimulation, other potential mechanisms may facilitate the relocation of ATR and RPA32. To study this sequence of events at greater temporal resolution live-cell imaging to observe the dynamic changes of RASSF1A, ATR, and RPA32 over shorter time scales would be required. In order to do this however, fluorescently tagged plasmid constructs need to be generated.

In this study, RASSF1A plays a role in promoting the formation of NAFs under replication stress. However, the specific mechanisms underlying this role remain to be further explored. On one hand, we found that the binding of RASSF1A to Filamin A increased, which suggests that RASSF1A may directly participate in the formation of NAFs structures, thereby facilitating NAFs formation. On the other hand, based on the findings reported by Maria Chatzifrangkeskou et al., RASSF1A plays a crucial role in regulating the nucleocytoplasmic shuttling of nuclear actin [18]. Therefore, it is also possible that RASSF1A itself or pRASSF1A may disrupt the equilibrium of actin shuttling, leading to perinuclear ACTIN aggregation, which in turn provides the conditions necessary for NAFs formation. This hypothesis still needs to be further verified, for example, by conducting cytoplasmic-nuclear fractionation experiments to detect whether the levels of nuclear and cytoplasmic actin change under HU treatment.

It is worth noting that, as highlighted by Maria Chatzifrangkeskou et al., MST2 plays a key role in the nuclear membrane localisation of RASSF1A [18]. We observed that after 4 hours of HU stimulation, the binding capacity between MST2 and RASSF1A remained unchanged, which may explain why RASSF1A did not exhibit significant translocation under HU stimulation. However, upon ATR inhibition, RASSF1 phosphorylation was markedly suppressed, and the MST2-RASSF1A interaction was significantly reduced, but only in the group subjected to 4 hours of HU stimulation. This suggests that the existence of other non-ATR-dependent mechanisms that could induce NAFs formation in the absence of DNA replication stress. Additionally, ATR-mediated RASSF1A phosphorylation may depend on the interaction between MST2 and RASSF1A. Therefore, further investigation into the dynamic behaviour of MST2 will be a critical focus in future studies.

It is emphasized that under replicative stress, ATR and RPA32 foci, or stress sites, tend to translocate to the nuclear periphery with prolonged HU treatment. This behaviour is beneficial for alleviating replicative stress and promoting damage repair [20]. From a physiological standpoint, this finding is conceptually similar to the role highlighted by Lopes et al., where nuclear actin polymerisation restricts the activity of PrimPol (a primase-polymerase) to coordinate the plasticity of replication forks [21].

In clinical samples, RASSF1A is frequently lost or silenced in cancers [14]. As previously described, our study revealed the dual regulatory role of RASSF1A in responding to mechanical and replicative stress signals. For instance, RASSF1A can respond to replicative stress by promoting the formation of NAFs to maintain genomic stability, thereby exerting a cancer-suppressive effect. Once RASSF1A is silenced or lost, the ability to withstand replicative stress is weakened, leading to increased genomic instability, which may further contribute to the development and progression of cancer.

However, several limitations exist in this study. Firstly, the phospho-RASSF1 antibody we used is not specifically targeted to RASSF1A and may also recognise isoforms such as RASSF1C. Consequently, the pRASSF1 levels detected in the WB may not accurately reflect the changes in pRASSF1A under HU stimulation. Secondly, since ATR activation and its functional execution mainly occur in the nucleus, conducting WB analysis directly on whole-cell lysates does not distinguish between the phosphorylation changes of nuclear and cytoplasmic RASSF1A. Thus, we cannot rule out the possibility that cytoplasmic RASSF1A translocation is involved in NAFs formation. Additionally, in the siRNA experiments, we lacked control groups, the control siRNA with 4-hour HU stimulation. In the ATR inhibition experiments, we lacked samples treated with VE-821 for different durations without HU stimulation. These

experiments require further replication and validation.

In summary, our results demonstrate that HU-induced replication stress in HeLa cells leads to the formation of nuclear actin filaments. Initially, ATR was diffusely distributed in the nucleus but, over time, formed complexes with RPA32 and migrated to the NE, coinciding with increased phosphorylated RASSF1A. Additionally, inhibition of ATR reduced NAFs and RASSF1A phosphorylation. SiRNA knockdown of RASSF1A also inhibited NAFs formation and HU-induced RPA32 aggregation. These findings suggest that ATR may facilitate the formation of nuclear actin filaments by promoting RASSF1A phosphorylation and its binding to filamin A, potentially aiding the translocation of replication stress sites to the nuclear periphery.

6. References

1. Brown, E.J. and D. Baltimore, *Essential and dispensable roles of ATR in cell cycle arrest and genome maintenance.* Genes Dev, 2003. **17**(5): p. 615-28.
2. Zou, L. and S.J. Elledge, *Sensing DNA Damage Through ATRIP Recognition of RPA-ssDNA Complexes.* 2003. **300**(5625): p. 1542-1548.
3. Cortez, D., et al., *ATR and ATRIP: partners in checkpoint signaling.* Science, 2001. **294**(5547): p. 1713-6.
4. Bermejo, R., et al., *The replication checkpoint protects fork stability by releasing transcribed genes from nuclear pores*. Cell, 2011. **146**(2): p. 233-46.
5. Kumar, A., et al., *ATR mediates a checkpoint at the nuclear envelope in response to mechanical stress.* Cell, 2014. **158**(3): p. 633-46.
6. Svitkina, T., *The Actin Cytoskeleton and Actin-Based Motility.* Cold Spring Harb Perspect Biol, 2018. **10**(1).
7. Baarlink, C., et al., *A transient pool of nuclear F-actin at mitotic exit controls chromatin organization.* Nat Cell Biol, 2017. **19**(12): p. 1389-1399.
8. Caridi, C.P., et al., *Nuclear actin filaments in DNA repair dynamics.* Nat Cell Biol, 2019. **21**(9): p. 1068-1077.

9. Caridi, C.P., et al., *Nuclear F-actin and myosins drive relocalization of heterochromatic breaks.* Nature, 2018. **559**(7712): p. 54-60.
10. Lamm, N., et al., *Nuclear F-actin counteracts nuclear deformation and promotes fork repair during replication stress.* Nat Cell Biol, 2020. **22**(12): p. 1460-1470.
11. Papaspyropoulos, A., et al., *RASSF1A uncouples Wnt from Hippo signalling and promotes YAP mediated differentiation via p73.* Nat Commun, 2018. **9**(1): p. 424.
12. Richter, A.M., G.P. Pfeifer, and R.H. Dammann, *The RASSF proteins in cancer; from epigenetic silencing to functional characterization.* Biochim Biophys Acta, 2009. **1796**(2): p. 114-28.
13. Mo, J.S., H.W. Park, and K.L. Guan, *The Hippo signaling pathway in stem cell biology and cancer.* EMBO Rep, 2014. **15**(6): p. 642-56.
14. Burbee, D.G., et al., *Epigenetic inactivation of RASSF1A in lung and breast cancers and malignant phenotype suppression.* J Natl Cancer Inst, 2001. **93**(9): p. 691-9.
15. Shivakumar, L., et al., *The RASSF1A tumour suppressor blocks cell cycle progression and inhibits cyclin D1 accumulation.* Mol Cell Biol, 2002. **22**(12): p. 4309-18.
16. Pefani, D.E., et al., *RASSF1A-LATS1 signalling stabilizes replication forks by restricting CDK2-mediated phosphorylation of BRCA2.* Nat Cell Biol, 2014. **16**(10): p. 962-71, 1-8.
17. Liu, J.S., S.R. Kuo, and T. Melendy, *DNA damage-induced RPA focalization is independent of gamma-H2AX and RPA hyper-phosphorylation.* J Cell Biochem, 2006. **99**(5): p. 1452-62.
18. Chatzifrangkeskou, M., et al., *RASSF1A is required for the maintenance of nuclear actin levels.* The EMBO Journal, 2019. **38**(16).
19. Jaalouk, D.E. and J. Lammerding, *Mechanotransduction gone awry.* Nat Rev Mol Cell Biol, 2009. **10**(1): p. 63-73.
20. Lamm, N., S. Rogers, and A.J. Cesare, *Chromatin mobility and relocation in DNA repair.* Trends Cell Biol, 2021. **31**(10): p. 843-855.
21. Palumbieri, M.D., et al., *Nuclear actin polymerization rapidly mediates replication fork remodeling upon stress by limiting PrimPol activity.* Nature Communications, 2023. **14**(1): p. 7819.